# Coupling of ultrasonic vibration and electrovibration for tactile stimulation

**Éric Vezzoli**[1], **Wael Ben Messaoud**[1,2], **Clément Nadal**[1], **Frédéric Giraud**[1], **Michel Amberg**[1], **Betty Lemaire-Semail**[1], **Marie-Ange Bueno**[2]

*1. Univ. Lille, Centrale Lille, Arts et Métiers Paris Tech, HEI, EA 2697 - L2EP
(Laboratoire d'électrotechnique et d'électronique de puissance)
59000 Lille, France*

*eric.vezzoli@ed.univ-lille1.fr*

*2. LPMT laboratory, University of Haute Alsace, 68093 Mulhouse, France*

*ABSTRACT. Electrovibration and squeeze film effect are two different principles, which modify the user's perception of a surface. The first one is generated by the polarization of a finger approaching a high voltage supplied plate, and the latter by the ultrasonic vibration of a plate. Their compatibility on the same stimulator will be presented in this paper and their concomitant use will be proven. A parametric study on electrovibration in function of the material choice and a first experimental investigation of the validity of the squeeze film effect hypothesis are performed. A description of the physical principle and the characteristics of each effect will be proposed and force measurements of their coupling will be presented.*

*RÉSUMÉ. L'électrovibration et l'effet squeeze film produit par vibration ultrasonique sont deux principes de stimulation tactile permettant de modifier la sensation de toucher d'un utilisateur explorant une surface plane. Le présent article s'attache à démontrer leur compatibilité sur un même stimulateur tactile lors d'une utilisation concomitante. Une description du principe physique et des spécificités de chacun des phénomènes sera entreprise et les résultats expérimentaux obtenus lors de leur association seront par ailleurs présentés.*

*KEYWORDS: tactile stimulators, ultrasonic vibration, squeeze film effect, electrovibration, haptic, tactile devices.*

*MOTS-CLÉS : stimulateur tactile, vibrations ultrasoniques, effet squeeze film, électrovibration, haptique, écrans tactiles.*

## 1. Introduction

During the last decades, a lot of attention has been paid to the role of touch in the human machine interaction for its relevance in the object identification and manipulation. The sensation of the correspondent action should be provided to the user to increase the quality of the interaction with the machine. Two kinds of stimulation are available concerning the finger: the local and the global stimulation. To each of them, a different class of tactile stimulator is referred. The former allows to render a localized sensation on the finger with a resolution comparable with the fingerprint. In this kind of stimulators, the finger is usually static and stimulated by the tactile feedback interface. This stimulation is generally based on a pillar matrix vibrating in the range of hundreds of Hertz with an amplitude of a few micrometers (Shimojo, 2004). The latter involves uniform stimulation of the fingertip. The finger should be in motion on the tactile stimulator to perceive the modulation of the stimulus. One class of these stimulator is based on the modulation of the friction between the finger and the surface; the ability to track the position of the finger thanks to its position sensing techniques leads to the generation of a spatio-temporal relation useful to generate texture (Biet *et al.*, 2008). Two technologies are available to modulate the friction between a surface and a finger. The first is called electrovibration ( Mallinckrodt *et al.,* 1953; Kaczmarek *et al.,* 2006; Bau *et al.,* 2010; Vezzoli *et al.,* 2014), it allows to increase the friction force between a finger and a surface thanks to electrostatic attraction. The second implies the ultrasonic vibration of a surface which reduces the friction between the two sliding objects, (Biet *et al*., 2007; Winter *et al.,* 2013; Ben Messaoud *et al.,* 2014;). These two physical phenomena concern a global modification of the friction between the finger and the surface. The interest around these two technologies has raised after the commercialization of the first touch-based devices. The absence of reliable haptic feedback in smartphones and tablets obliges the users to pay continuous attention to the screen while interacting with the devices. These two technologies have shown the promising opportunity to be coupled with capacitive touchscreens and their superior performances to render haptic feedback has pushed the interests of high-tech producers.

The electrovibration was the first of these technologies to be implemented in tactile devices (Mallinckrodt *et al.,*1953). The original idea was to generate a dense matrix of electrodes covered with an insulator to generate localized attraction to stimulate locally the finger. Unfortunately, this approach didn't work because of the impossibility to distinguish the active electrode to the others. The acquisition of the finger position became then relevant, the developing of resistive and capacitive position sensor helped to resolve the problem. The further developing of transparent sensors allowed to realize the firsts transparent stimulators (Bau *et al.,* 2010).

The friction reduction by ultrasonic vibration has been firstly described by Watanabe *et al.* (Watanabe *et al.,* 1995): they firstly explained the reduction of the friction by a generation of a pressured gas film between the finger and the plate. The

analytic development of the concept and evolution of the performances of the devices has been then performed in (Biet *et al.,* 2007; Winfield *et al.,* 2007).

In this paper, the coupling of the two techniques is presented. Firstly introduced by (Giraud *et al.,* 2013), the work is extended here to compare the modelling and experimental results obtained with the two friction modulation principles; moreover, a parametric study on the performance of the electrovibration is proposed for its first application in a prototype of a mobile consumer device and its possible future relevance in the consumer world.

## 2. Explanation and model of the two friction modulation principles

### 2.1. Ultrasonic vibrations

#### 2.1.1. Principle

In this section, the principles at the basis of the friction reduction with ultrasonic devices are recalled. The first explanation of the friction reduction between the finger and an ultrasonic vibrating plate relied on the squeeze film effect. This phenomenon occurs when the air gap between two plates, – one vibrating at ultrasonic frequency, the other one fixed – is compressed and decompressed periodically by the motion of the ultrasonic vibrating plate. The non-linear relation between the volume of trapped gas between the two plates and the pressure leads to an average overpressure of the gas between the two surfaces. In Figure 1 is reported a study case where two flat plates are facing, the trapped air between the two is cyclically compressed and decompressed resulting in an average pressure bigger than the ambient one (Biet *et al.,* 2007). This phenomenon is supposed to happen between a finger and a vibrating plate, in that case, the trapped gas in overpressure introduce a sustain force under the finger pad which reduces the applied normal force by the finger. The result is a sensation of smoother surface when the finger slides on the vibrating plate.

The sustain provided by the overpressure under the finger is the factor leading to the friction reduction (Figure 2). Evidence of this phenomenon has been observed in (Dai *et al.,* 2012) during their experimental analysis. This phenomenon can be induced by the vibration of a surface of some micrometers at ultrasonic frequency (>25 kHz). To perform this movement, the mechanical resonance of a rigid plate is induced in the ultrasonic bandwidth, reducing by that way the required energy. As a consequence, a standing wave is generated. To put the surface in motion, a matrix of piezoelectric ceramics is glued under the vibrating plate. The power supply of the actuators is modulated as a sinusoidal profile at the frequency correspondent to the excited mode of vibration of the device. The vibration mode is defined with a finite element software to correctly position the piezoelectric ceramics in the antinodes of the modes to obtain an optimized electro-mechanical coupling. A cartography of a standing wave and a picture of the matrix of piezoelectric ceramics are reported in

Figure 3. The current design of the plate is based on the STIMTAC, developed by Amberg *et al.* (Amberg *et al.,*. 2011). It may be noted that the perceptual bandwidth of the mechanoreceptors in the skin is far below the provided stimulation (<1 kHz), so the finger is just able to perceive the envelope of the ultrasonic wave generated (Maeno *et al.,* 2006).
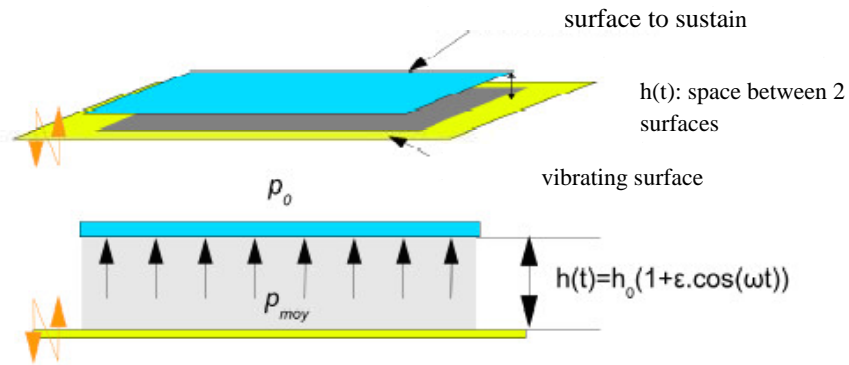


surface to sustain

h(t): space between 2 surfaces

vibrating surface

$p_o$

$p_{moy}$

$h(t)=h_0(1+\varepsilon.\cos(\omega t))$

*Figure 1. Working principle of the squeeze film effect: the trapped air between the two surfaces, following the cyclical compression performed by the moving lower plate, results in an average pressure bigger than the atmospheric one leading to net support of the upper surface*
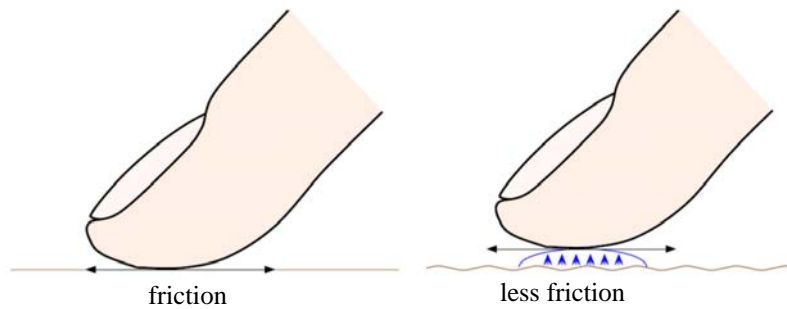


friction                less friction

*Figure 2. Influence of the squeeze film effect. The induced over pressure by the ultrasonic vibration sustains the finger pad during the sliding and reduces the friction between the finger and the surface*
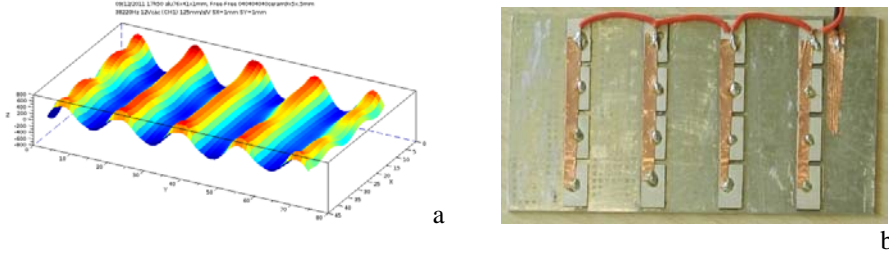
*Figure 3. A cartography of the vibration mode of the plate (a),*
*disposition of the piezoceramics glued on the back part of the plate (b)*

### 2.1.2. Modeling of the phenomenon

In the model proposed in (Biet *et al.,* 2007), the reduction of the friction coefficient imputed to the ultrasonic vibration through the squeeze film effect can be determined by the following relation:

$$\frac{\mu - \Delta\mu}{\mu} = \frac{F_s}{F_n} \tag{1}$$

where $F_n$ and $F_s$ are the normal force applied from the finger and the sustain force of the overpressure induced by the squeeze film effect, $\mu$ is the Coulomb friction coefficient without any squeeze effect, and $\Delta\mu$ is the difference between the fiction coefficient without squeeze effect and the actual friction coefficient with squeeze effect: $\Delta\mu = \mu(W = 0) - \mu(W)$. $F_s$ is temporally averaged over a vibration cycle and over the fingertip area. $F_s$ can be calculated through the following expression:

$$F_s = \frac{p_0 A}{l_0 T} \int_0^T \int_{-l_0/2}^{l_0/2} [\bar{P}_\infty(x,t)\text{-}1] dx dt \tag{2}$$

Where $\bar{P}_\infty(x,t)$ is the air pressure between the finger and the vibrating plate normalized to the atmospheric pressure. The proposed model can take into account the vibration amplitude $h_v$ of the flexural wave, the roughness of the plate with $h_r$, and the geometry of the fingerprints supposed to have a sinusoidal profile with $L_e$ period and $h_e$ amplitude, as represented in Figure 4.
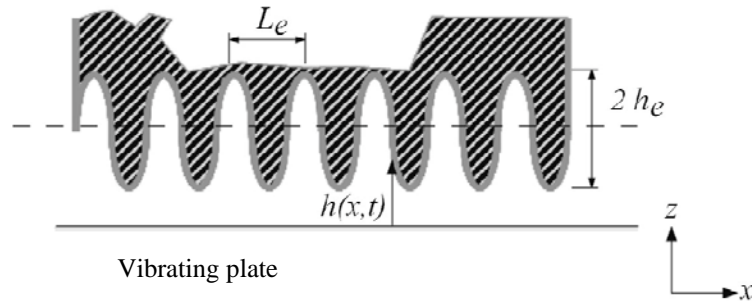
*Figure 4. Geometry of the fingerprints considered in the model of (Biet et al., 2007)*

From this modeling, it is possible to compute the thickness of the air film between the finger and the plate:

$$h(x,t) = h_r + h_v[1 + \cos(\omega t)] + h_e[1 + \cos(kx)] \qquad (3)$$

where $k = 2\pi / L_e$. With the Navier-Stokes equation, and the hypothesis of isothermal transformation proposed in their work. It is possible to show that the thickness of the air film $h(x,t)$ and the associated pressure $p(x,t)$ can be considered under the assumption of an isotherm transformation. This leads to the possibility to describe the system with the unidimensional Raynolds equation:

$$\frac{\partial}{\partial X}\left[H^3(X,T)P(X,T)\frac{\partial P}{\partial X}(X,T)\right] = \sigma\frac{\partial}{\partial T}[P(X,T)H(X,T)] \qquad (4)$$

Where $H(X,T) = h(x,t)/h_0$ with $h_0 = h_r + h_v + h_e$ and $P(x,t) = p(x,t)/p_0$ are the nondimensional thickness of the air film and the normalized pressure of the fluid. These values are in function of the variable $X = x/l_c$ and $T = \omega t$. The variable $\sigma$ appeared in Equation (4) is called squeeze number, and it is defined by:

$$\sigma = \frac{12\eta\omega A}{p_0(h_r + h_v + h_e)^2} \qquad (5)$$

where $\eta$ is the air viscosity. This quantity represents the compressibility of the fluid between the finger and the plate in vibration. For big values of $\sigma$, the fluid is considered incompressible instead, for small values it acts like a spring. Following, it is supposed that the fluid presents a big squeeze number to introduce the simplification of $\sigma \to +\infty$ (this hypothesis can be justified if $\sigma > 10$ (Biet *et al.,* 2007; Winter *et al.,* 2013). Introducing this hypothesis it is possible to compute the profile of the pressure under the fingertip:

$$\bar{P}_\infty(x,t) = \frac{[1 + \delta \cos(kx)] \sqrt{\left[1 + \delta \cos\left(\frac{kl_0}{2}\right)\right]^2 + \frac{3}{2}\varepsilon^2}}{\left[1 + \delta \cos\left(\frac{kl_0}{2}\right)\right][1 + \delta \cos(kx) + \varepsilon \cos(\omega t)]}$$

(6)

where $\delta = h_e/h_0$ and $\varepsilon = h_v/h_0$. Introducing the previous Equation into (2), leads to the expression (1). It has been performed some tribological measurement thanks to the tribometer detailed in (Vezzoli *et al.,* 2014) to assess the validity of the proposed theoretical calculation. In table 1, the parameters used for the theoretical comparison are reported.

*Table 1. Parameters to model the friction reduction imposed*
*by the squeeze film effect*

|  | | Definition | Value | Units |
|---|---|---|---|---|
| $h_r$ | | Absolute roughness of the plate (Ra) | 1.8 | µm |
| $h_e$ | | Amplitude of the finger prints | 50 | µm |
| $L_e$ | | Spatial period of the fingerprints | 350 | µm |
| $f_r$ | | Frequency of the mode excited | 38220 | Hz |
| $\lambda$ | | Spatial period of the excited mode | 0.8 | cm |
| $F_n$ | | Normal force applied by the finger | [0.2, 0.4] | N |
| $\eta$ | | Dynamic viscosity of the air | $1.85 \times 10^{-5}$ | Pa.s |
| $p_0$ | | Atmospheric pressure | $10^5$ | Pa |

The theoretical results are reported later in Figure 8 which shows a strong dependence of the friction modulation with the applied force and the vibration amplitude. For example, for an applied force of 0.2 N, a vibration amplitude above 2 µm will be necessary to induce a complete acoustic levitation.

### *2.2. Electrovibration*

#### *2.2.1. Principle*

In this section, the electrovibration technology is explained. The electrovibration is based on the polarization of a finger approaching a high voltage supplied plate. While sliding on a device equipped with this technology, the increased normal load provided by electrostatic interaction contributes to the generation of the lateral force.

The modulation of the force is weak, but is compatible with the forces applied by the finger during the touch-sensing action (Adams *et al.,*. 2013). The modulation of the provided voltage to the polarizing plate determines a modulation of the friction between the finger and the plate. The working principle of the electrovibration is presented in Figure 5.
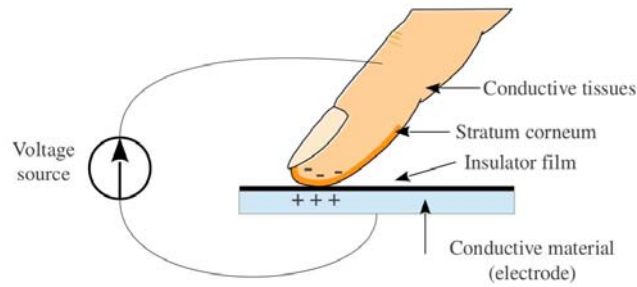


*Figure 5. Working principle of electrovibration (Vezzoli* et al., *2014)*

It is possible to show that the electrostatic force between the finger and the plate assumes this expression (Vezzoli *et al.,* 2014):

$$f_e(t) = \frac{\varepsilon_0 \, A \, v_e^2(t)}{2(h_i + h_s)\left(\frac{h_i}{\varepsilon_i} + \frac{h_s}{\varepsilon_s}\right)}$$

(7)

where $h_i$ et $h_s$ are thickness of the insulator and the stratum corneum and, $\varepsilon_i$ et $\varepsilon_s$ their relative permittivity, $\varepsilon_0$ is the permittivity of the air and A is the contact area between the finger and the plate. The electrostatic force is dependent of the thickness and the composition in terms of water and lipid ratio of the stratum corneum, which is strongly variable between different subjects. This means that different users will experience different forces while interacting with the tactile device. The electrical properties of the human skin are strongly dependent on the frequency of the applied voltage; this can affect the generation of the force. The calculus of Equation (7) and the influence of the variability of the properties of the human skin are described in detail in (Vezzoli *et al.,* 2014).

### 2.2.2. Modeling of the phenomenon

From Equation (7), it is possible to evaluate the average electrostatic force imposed by the electrovibration. It is necessary to compute the effective voltage $v_e(t)$ acting on the fingertip in function of the applied voltage $v(t)$ between the body and the plate. In (Vezzoli *et al.,* 2014) it has been shown that the voltage $v_e(t)$ across the stratum corneum could be written as:

$$v_e(j\omega) = \frac{j\omega\tau}{1 + j\omega\tau} v(j\omega) \tag{8}$$

where $\tau = R_s C_s = \varepsilon_0 \varepsilon_s \rho_s$ with $\rho_s$ the resistivity of the stratum corneum and $\varepsilon_s$ the permittivity of the stratum corneum. The reported model is valid under the assumption that the capacitance associated to the insulator on the stimulating device is smaller compared to the one of the finger, $C_i \ll C_s$. It has to be noticed that the electrical characteristics of the stratum corneum reported in (Yamamoto *et al.*, 1976) strongly depend of the frequency of the exciting voltage. The temporal expression of the effective voltage is not straightforward, but considering a sinusoidal signal simplifies the calculus. It can be described by $v(t) = V_m cos(\omega t)$ where $\omega = 2\pi f$ with f the frequency of the imposed signal. The effective voltage $v_e(t)$ can be then expressed in the time domain:

$$v_e(t) = V_m \frac{\omega\tau}{\sqrt{1 + (\omega\tau)^2}} cos\left[\omega\tau + \frac{\pi}{2} - arctan(\omega\tau)\right] \tag{9}$$

Consequentially, the average value of the electrostatic force generated by the electrovibration assumes the expression:

$$F_e = \frac{\varepsilon_0 A V_m{}^2}{4(h_i + h_s)\left(\frac{h_i}{\varepsilon_i} + \frac{h_s}{\varepsilon_s}\right)} \frac{(\omega\tau)^2}{1 + (\omega\tau)^2} \tag{10}$$

It may be noted that this force strongly depends on the user finger characteristics, the voltage supply, the frequency supply and the insulator properties. To have an idea, we have reported in Table 2 some parameters corresponding to average values for the finger and real values for our tactile stimulator.

Starting from the parameters reported in Table 2, corresponding to the characteristic of the device developed for the measurements, the average electrostatic force theoretically expected is $F_e = 0.056\ N$, which may be detected by the finger through the tangential force variation induced.

*Table 2. Parameters of the electrovibration device and average parameters for the finger*

|  | Definition | Value | Units |
|---|---|---|---|
| $h_i$ | Thickness the plastic film | 90 | $\mu m$ |
| $h_s$ | Average thickness of the statum corneum | 350 | $\mu m$ |
| $A$ | Average apparent surface in contact | 1 | $cm^2$ |
| $\varepsilon_i$ | Relative permittivity of the plastic film | 3.35 | |
| $\varepsilon_s$ | Average relative permittivity of the stratum corneum at 440 Hz | 2340 | |
| $\rho_s$ | Average resistivity of the stratum corneum at 440 Hz | $3.0 \times 10^4$ | $\Omega m$ |
| $V_m$ | Amplitude of the power supply | 2000 | $V$ |
| $f$ | Frequency of the applied tension | 440 | $Hz$ |

## 3. Technologies coupling

### 3.1. Principle

According to the complementarity of the two principles for friction modulation previously introduced, it is possible to propose a modeling of the two coupled technologies assuming that the extra normal force induced by electrovibration does not modify the reduction of the friction coefficient performed by the ultrasonic vibrations. It is possible to implement a modeling based on the the Coulomb friction law may be adapted as:

$$F_t = (\mu\text{-}\Delta\mu)(F_n + F_e) \tag{11}$$

where $F_t$ is the tangential force, $F_n$ is the normal force applied by the finger, $F_e$ is the electrostatic force imposed by the electrovibration and $\Delta\mu$ is the modulation of the friction coefficient performed by the ultrasonic vibrations.

### 3.2. Experimental setup

To evaluate the coupling of the two technologies, the following experimental setup is elaborated. The hybrid tactile stimulator is based on a modified version of the STIMTAC (Amberg *et al.,* 2011), where the tactile plate and the inverter which supplies it have been electrically decoupled. The interface is composed of an aluminum plate covered by a plastic insulator $90 \, \mu m$ thick. In this way, it was possible to insert a high voltage amplifier to polarize the plate, Figure 6a. The force measurement is performed with a six axis force sensor (nano43, ATI, USA). With

this experimental setup it is possible to perform simultaneously the measurements of the tangential and normal forces. To measure the effective parameter modifying the friction, the vibration amplitude of the plate is measured with a laser vibrometer (OVF-5000, Polytech, Germany) focused on the tactile plate, and the voltage applied to induce the electrovibration is recorded. Data are collected through an oscilloscope (TDS3014B, Tektronix, USA) and then post processed.
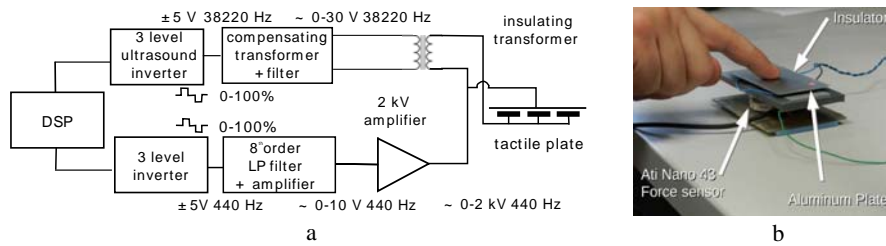


*Figure 6. Block scheme of the device developed to perform the measurements (a), device mounted on the force sensor to perform measurements (b), the red spot on the tactile plate is the focus of the laser vibrometer*

### 3.3. Results

#### 3.3.1. Evaluation of ultrasonic friction reduction

The experimental validation of the friction reduction induced by the ultrasonic vibration and modeled with the squeeze film effect theory has been performed in active exploration by a user. He gave his informed consent on the deployment of the experiment. An initial period of training was necessary in order to ensure the stability of the exploration speed and the normal force imposed by the finger. These data were provided via a visual interface to the user. The experiment has been performed with an exploration speed of 30mm/s and a normal force variable form 0.2 to 0.4N. Before each measurement, the tactile plate has been cleaned and the exploration was allowed just for 30 seconds, followed by 30 seconds of break to let the finger dry. This precaution was necessary because the humidity of the finger can influence its tribological behavior. Before the starting of the experiment the finger was cleaned and accurately dried with talcum powder. The results of the performed measurements are reported in Figure 7.

The friction reduction in ultrasonic devices have been explained with the squeeze film effect since the beginning (Watanabe *et al.*, 1995; Biet *et al.*, 2007), but an experimental assessment on the validity of the model have never been performed. The measure in Figure 7 shows that, on one hand, the vibration amplitude is able to reduce the friction between the plate and the finger, on the other hand, the experimental points seem to reach an asymptote for high vibration amplitude, that means a complete acoustic is impossible to induce, even with a vibration amplitude

far greater than the one predicted by the model. The reason and the analysis of this result are no concern of this work. It is just possible just to conclude that a modeling based on the squeeze film effect cannot explain all the features of the frictionmodulation induced in ultrasonic devices. Other possible explanations of the phenomenon have been proposed in (Vezzoli *et al*., 2015), an accurate modelling of the phenomenon is the next step of this work.
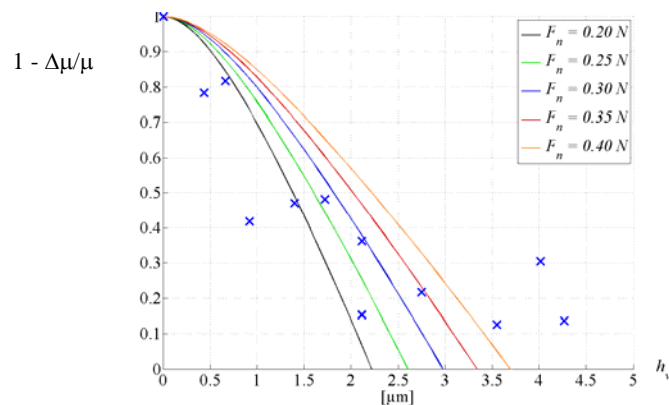


*Figure 7. Measured friction reduction imposed by the ultrasonic vibrations in function of the vibration amplitude of the plate (x dots). The colored lines represent the predicted friction reduction by the squeeze film effect for the measured experimental parameters of the system*

### 3.3.2. Evaluation of friction force increase due to electrovibration effect

The aim of this paragraph is to perform an analysis about the accuracy of our modelling for electrovibration and to discuss about the variability of the induced electrostatic force with such parameters as the applied voltage, the supply frequency, the stratum corneum thickness or the insulator properties.

First, to check the accuracy of the modelling proposed in 2.2.2, we compute the electrostatic force $F_e$ as a function of the supply frequency, for different values of the stratum corneum thickness, in the range given by (Fruhstorfer, 2000). The other conditions are equal to the experimental ones described in (Meyer *et al.,* 2013). Then, using Equation (11), it is possible to compute the electrostatic force. The results are reported in Figure 8.

We can see that the variability of the thickness of the stratum corneum plays a major role in the determination of the electrostatic force induced on the fingertip. Moreover, the experimental results obtained by (Meyer *et al.,* 2013) are in agreement with the modelling proposed in this paper.
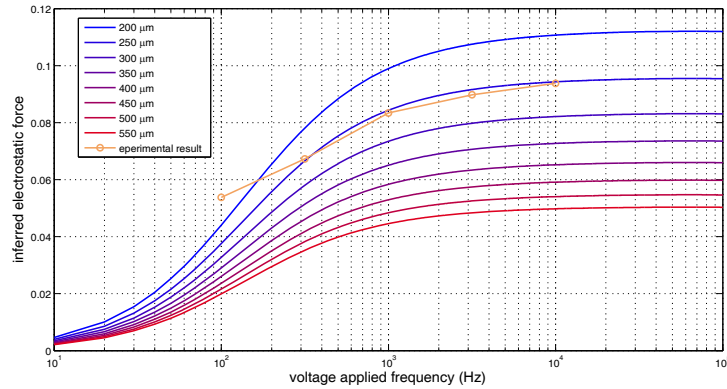
*Figure 8. Variability of the electrostatic force imposed by the electrovibration effect for different thicknesses of the stratum corneum, the experimental data are taken from (Meyer et al., 2013): $v_{max}$=140v, frequency: from 100 to 10000 Hz, insulator thickness: 1µm and permittivity: 3.4*

Second, the properties of the insulator are investigated thanks to our modelling in order to highlight the quality needed to perform an accurate electrostatic force. The material properties of the insulator play an important role for the determination of the electrostatic force induced by the device. The choice of the insulator between the tactile plate and the finger needs also to commit requirements of wear resistance and in the case of application to tactile screens, to be transparent. The dependence of the electrostatic force induced in the finger as a function of the insulator thickness for a sinusoidal voltage at 500Hz, 140V max. is reported in Figure 9. Three transparent reference materials are also reported: silicium dioxide (glass), zirconium oxide and zirconium dioxide (zircona in crystalline form). These materials are transparent, and ITO films can be deposed over them (Kaneko *et al.,* 2012; Ohta *et al.,* 2000) for typical use in tactile screens.

From Figure 9, we can conclude first that for a given voltage, the thinnest the insulator is, the greatest the force is. Second, the insulator permittivity has also to be high in order to maximize the force, for a given voltage and a given thickness. Considering the three transparent materials reported in Figure 9, if we want to reach a force around 0.03N which is three times the minimal force we can experimentally detect with a sliding finger, we have to use for $ZnO_2$ a 8,5 µm thick layer of insulator, for ZnO, a 2.5µm layer and for $SO_2$, lees than 1 µm layer. Of course, wear consideration has to be taken into account to avoid a too thin layer of insulator. For a given value of permittivity, then the applied voltage should be increased in order to reach the desired force.
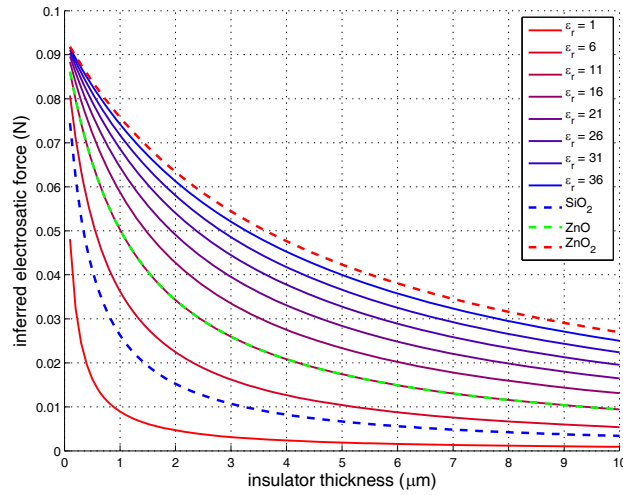
*Figure 9. Dependence of the induced electrostatic force with the dielectric constant of the insulator, from 1 to 36, as a function of different insulator thickness. The dotted lines correspond to some selected materials*
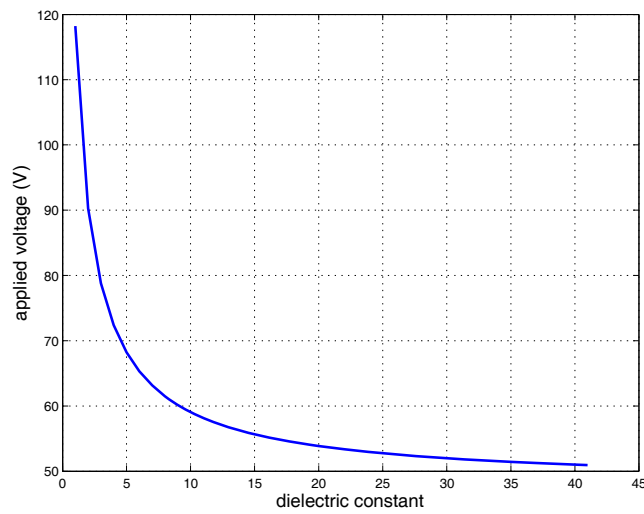


*Figure 10. Required voltage to induce an electrostatic force modulation of 0.01N with an insulator thickness of 1µm and a voltage frequency of 500Hz in function of the dielectric constant*

An analysis of the voltage limits to obtain a minimal stimulation with $F_e$=0.01N is interesting to establish the lower limit of voltage to be used for different material

permittivity. The computation of this voltage limit from Equation (11) is reported in Figure 10 for an insulator thickness of 1μm and a signal frequency of 500Hz. This analysis can lead to specifications for tactile feedback display design operating with electrovibration.

### 3.3.3. Evaluation of the coupling of the two technologies

In this section, the results of the coupling of the two tactile stimulations are presented. To confirm the increased range of sensation that the two coupled technologies can provide to the user, they were initially tuned to induce a similar friction modulation ($|\Delta F_t(EV)|=|\Delta F_t(UV)|$) on the finger. Then they were applied to the moving finger in opposition and the resultant force has been recorded by the force sensor. In Figure 11 the obtained results are reported. The experiment was done in active exploration by the user which performed a period of training to maintain the speed as well as the normal force reasonably constant during the exploration. The subject gave his informed consent to the performing of the experiment and didn't suffer from physiological or cognitive deficits that might alter his/her tactile perception or judgment.
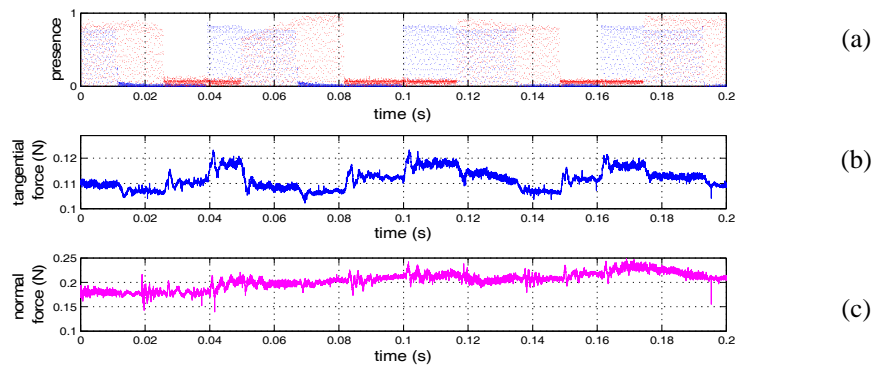


*Figure 11. Results of the measures performed with the two coupled technologies. Presence of the effect, in red ultrasonic vibration and in blue electrovibration (a), instantaneous tangential force (b), normal force applied by the finger (c)*

At each transition between different states, the tangential or friction force responds with a step change, without affecting the evolution of the normal force, which remains constant. It has to be noted that it is impossible to distinguish from the tangential force the presence of both effects or the absence of the friction modulation. It is noteworthy that it is possible to increase or decrease the friction between the finger and the plate from its original value.

To validate the complementarity of the two effects, Figure 12 illustrates the evolution of the tangential force as a function of simultaneous presence or absence

of both effects for a constant normal force applied by the finger (in the order of 0.2N).

This measure confirms that it is possible to completely compensate the effect of the friction increase due to electrovibration with the friction reduction due to ultrasonic vibrations. Figure 13 illustrates the case where the effects are applied against phase with the normal force still maintained around 0.2 N. The increased range of modulation which is possible to induce with the coupled techniques is clear.
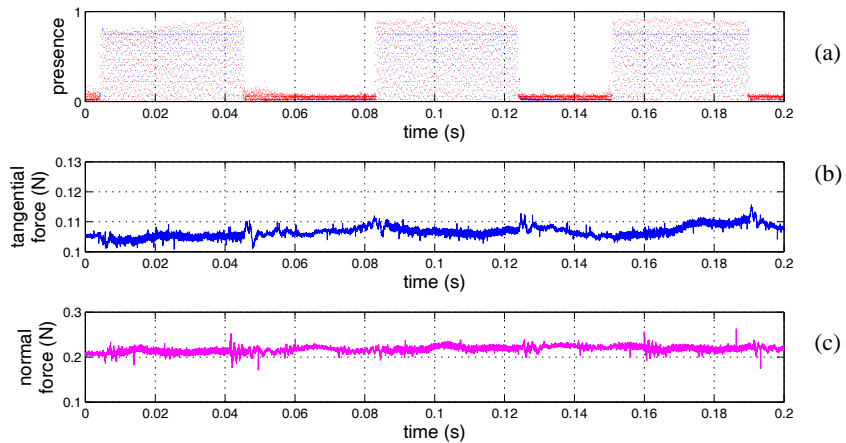


*Figure 12. Simultaneous presence of the electrovibration (blue) and ultrasonic vibrations (red) (a), tangential force (b), normal force applied from the finger (c)*
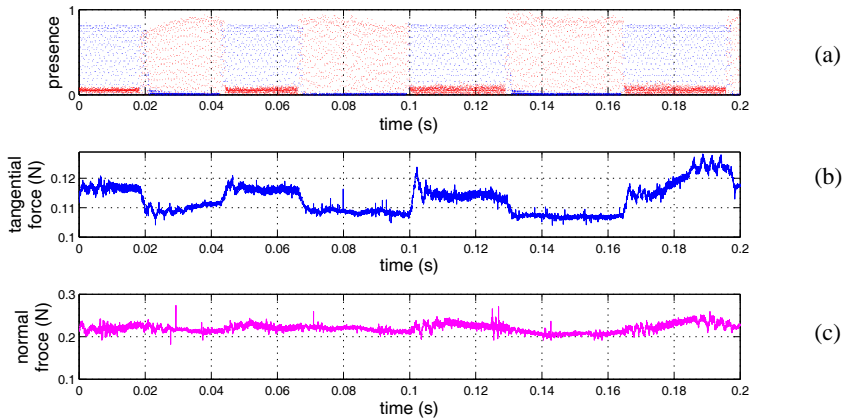


*Figure 13. Alternative presence of the electrovibration (blue) and ultrasonic vibrations (red) (a), tangential force (b), normal force applied from the finger (c)*

The two phenomena act in opposition, the ultrasonic vibration reduces the friction whereas the electrovibration increases it. The measures, Figure 11, 12 and 13, have been performed for 0°, 90° and 180° phase shift between the two signals. The two effects have been singularly tuned on the participant finger to induce the same amount of modulation for the applied speed and force. For a 0° phase shift, if the relation (11) is valid, a complete compensation of the lateral force effect is expected. The behavior reported in Figure 12 confirms the predicted behavior, the lateral force is maintaining a constant behavior independently to the presence of the stimulus. A 90° phase shift modulation generates a staircase stimulation, Figure 11, where cyclically the effects are absent (no modulation of the lateral force), electrovibration alone is applied (increased lateral force), both stimulations are applied (compensated modulation) and ultrasonic vibration alone is applied (decreased lateral force). A modulation in opposition, Figure 13, shows a greater modulation at every half period, inducing a bigger sensation than a single effect applied.

This validation indicates that the range of sensation induced with friction modulation devices can be expanded by the application of the two effects on the same device. The increased stimulation range leads to the possibility to reproduce sensation of surface with bigger or smaller friction then the stimulator one.

## 4. Conclusion

In this work, the coupling of two different friction modulation techniques has been analyzed with a focus on the increment of sensation that they can provide together. A first experimental validation of the squeeze film hypothesis has been performed rising questions on its validity. An analysis of the first prototype of tactile display committing the integration needed in the mass market has been carried out and leads to different solution proposals to reduce the required voltage for performing the stimulations.

## Bibliography

Adams M. (2013). Finger Pad Friction and Its Role in Grip and Touch. *Journal of The Royal Society Interface,* vol. 10, n° 80, p. 20120467.

Amberg M. (2011). STIMTAC: A Tactile Input Device with Programmable Friction. In *Proceedings of the 24th Annual ACM Symposium Adjunct on User Interface Software and Technology*.

Bau O. (2010). TeslaTouch: Electrovibration for Touch Surfaces. In *Proceedings of the 23Nd Annual ACM Symposium on User Interface Software and Technology*, p. 283-92.

Ben Messaoud W. (2014). Closed-Loop Control for Squeeze Film Effect in Tactile Stimulator. In *Proceedings of the 2014 international Conference and exhibition on new actuators and drives, Actuator 2014*. Bremen, Germany.

Biet M. (2008). Discrimination of Virtual Square Gratings by Dynamic Touch on Friction Based Tactile Displays. *symposium on Haptic interfaces for virtual environment and teleoperator systems, 2008*, p. 41-48.

Biet M. (2007). Conception et contrôle d'actionneurs électro-actifs dédiés à la simulation tactile, PhD Thesis, Université Lille1.

Biet M. (2007). Squeeze film effect for the design of an ultrasonic tactile plate *IEEE Transactions on Ultrasonics, Ferroelectrics, and Frequency Control,* vol. 54, n° 12, p. 2678-2688.

Dai X. (2012). A surface-haptic device that produces lateral forces on a bare finger. *2012 IEEE Haptics Symposium (HAPTICS)*, p. 7-14.

Fruhstorfer H. (2000). Thickness of the Stratum Corneum of the Volar Fingertips. *Clinical Anatomy,* vol. 13, n° 6.

Giraud F. (2013). Merging two tactile stimulation principles: electrovibration and squeeze film effect. *World Haptics Conference (WHC),* p. 199-203.

Kaczmarek, K.A. (2006). Polarity Effect in Electrovibration for Tactile Display. *IEEE Transactions on Biomedical Engineering,* vol. 53, n° 10, p. 2047-2054.

Kaneko S. (2012). Epitaxial Indium Tin Oxide Film Deposited on Sapphire Substrate by Solid-Source Electron Cyclotron Resonance Plasma. *Japanese Journal of Applied Physics,* vol. 51, n° 1.

Maeno T. (2006). Tactile Display of Surface Texture by use of Amplitude Modulation of Ultrasonic Vibration. *2006 IEEE Ultrasonics Symposium.*

Mallinckrodt E. (1953). Perception by the skin of electrically induced vibrations. *Science,* vol. 118, p. 277-78.

Meyer D.J. (2013). Fingertip friction modulation due to electrostatic attraction . In *World Haptics Conference (WHC),* 2013, p. 43-48.

Ohta H. (2000.). Highly electrically conductive indium–tin–oxide thin films epitaxially grown on yttria-stabilized zirconia (100) by pulsed-laser deposition. *Applied Physics Letters,* vol. 76, n° 19, p. 2740-2742.

Shimojo M. (2004). An Approach for Direct Manipulation by Tactile Modality for Blind Computer Users: Principle and Practice of Detecting Information Generated by Touch Action. *Computers Helping People with Special Needs*, Springer Berlin Heidelberg.

Vezzoli E. (2014). Electrovibration Modeling Analysis. *Haptics: Neuroscience, Devices, Modeling, and Applications.* Springer Berlin Heidelberg.

Vezzoli E. (2015) Role of Fingerprint Mechanics and Non-Coulombic Friction in Ultrasonic Devices. *IEEE-World Haptics Conference.*

Watanabe T. (1995). A method for controlling tactile sensation of surface roughness using ultrasonic vibration. *1995 IEEE International Conference on Robotics and Automation, 1995 Proceedings*, vol. 1, p. 1134-1139.

Winfield L. (2007). T-PaD: Tactile Pattern Display through Variable Friction Reduction. *EuroHaptics Conference, 2007 and Symposium on Haptic Interfaces for Virtual Environment and Teleoperator Systems. World Haptics 2007. Second Joint*, p. 421-426.

Winter C. (2013). Optimal design of a squeeze film actuator for friction feedback. In *Electric Machines Drives Conference (IEMDC), 2013 IEEE International*, p. 1466-1470.

Yamamoto T. (1976). Electrical Properties of the Epidermal Stratum Corneum. *Medical and Biological Engineering,* vol. 14, n° 2, p. 151-58.